ChemComm

RSC Publishing

COMMUNICATION

View Article Online
View Journal | View Issue

Pluronic polymer capped biocompatible mesoporous silica nanocarriers†

Cite this: *Chem. Commun.*, 2013, **49**, 9782

Received 5th August 2013,
Accepted 20th August 2013

DOI: 10.1039/c3cc45967e

www.rsc.org/chemcomm

Adem Yildirim,*[ab] Gokcen Birlik Demirel,[bc] Rengin Erdem,[ab] Berna Senturk,[ab] Turgay Tekinay[ab] and Mehmet Bayindir*[abd]

A facile self-assembly method is described to prepare PEGylated silica nanocarriers using hydrophobic mesoporous silica nanoparticles and a pluronic F127 polymer. Pluronic capped nanocarriers revealed excellent dispersibility in biological media with cyto- and blood compatibilities.

The high surface area and pore volume, good chemical stability and ease of surface functionalization of mesoporous silica nanoparticles (MSNs) make them promising materials for biological applications as drug carriers and theranostic agents.[1,2] In addition silica based materials are generally accepted as biocompatible materials by the U.S. Food and Drug Administration (FDA). However, recent studies demonstrated their potential *in vitro* and *in vivo* toxicity, especially when their size is reduced to the nano scale.[3,4] Although the toxicity of silica based nanomaterials depends on several factors including particle size, shape, surface chemistry and porosity,[5–7] there is a general consensus that chemical structure of the surface is the predominant factor which determines the interactions with biological systems.[8] The surface of bare silica is covered with negatively charged silanol groups, which can electrostatically interact with positively charged tetraalkylammonium moieties of the cell membrane and can lead to cytotoxicity by membranolysis or inhibition of cellular respiration.[8,9] Also, rapid aggregation of silica based nanoparticles in biological media can result in mechanical obstruction in the capillary vessels of several vital organs, leading to organ failure and even death.[10,11] Therefore, replacing the surface silanol groups with biocompatible molecules is essential to improve the biocompatibility of MSNs.

Among numerous polymeric or organosilane surface modification ligands, polyethylene glycol (PEG) is the mostly used one due to its well established biocompatibility, hydrophilicity, and antifouling properties.[12] However, the PEGylation process has some limitations; (i) it mostly requires tedious organic synthesis and surface modification[13] and (ii) pores of MSNs may be closed by the long PEG polymer chains, which can hinder the drug loading process. To overcome these limitations, here we report a facile self-assembly method using octyl modified hydrophobic MSNs and an amphiphilic block copolymer (F127). F127, a FDA approved biocompatible pluronic polymer, contains two hydrophilic PEG blocks and a hydrophobic polypropylene oxide (PPO) between the two PEG blocks.[14] When the powder of hydrophobic MSNs is added into the F127 solution they are easily transferred into water by self-assembly of F127 molecules onto the MSN surface through the hydrophobic interaction between the PPO block of F127 and surface octyl groups of the MSNs (Scheme 1). In addition, cargo loaded and PEGylated MSNs can be simply prepared by loading the hydrophobic MSNs before the F127 capping process. The F127 capped particles are dispersible in both water and phosphate buffered saline (PBS), whereas uncapped MSNs are easily aggregated and precipitated. The improved biocompatibility of F127 capped MSNs was demonstrated using cytotoxicity, hemolytic activity and thrombogenicity assays. Lastly, cargo release kinetics of PEGylated MSNs was investigated.

Octyl modified MSNs (O-MSN) were prepared *via* respective condensation of tetraethyl orthosilicate (TEOS) and octyltriethoxy silane (OTS) monomers in a one-pot reaction.[15–17] After polymerization of TEOS and formation of initial MSNs, OTS monomers were added in order to obtain hydrophobic coatings on MSNs. Also, for

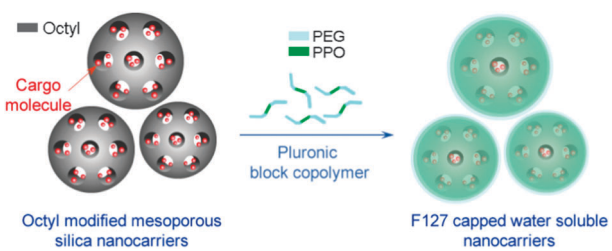

Scheme 1 Schematic representation of F127 capped MSN preparation.

[a] *Institute of Materials Science and Nanotechnology, Bilkent University, 06800 Ankara, Turkey. E-mail: ademy@bilkent.edu.tr*
[b] *UNAM-National Nanotechnology Research Center, Bilkent University, 06800 Ankara, Turkey*
[c] *Department of Chemistry, Gazi University, Polatlı, 06900 Ankara, Turkey*
[d] *Department of Physics, Bilkent University, 06800 Ankara, Turkey. E-mail: bayindir@nano.org.tr*

† Electronic supplementary information (ESI) available: Experimental details and general procedures, particle size distributions, surface area and pore volume analysis, TGA results, and the effect of washing on average particle size. See DOI: 10.1039/c3cc45967e

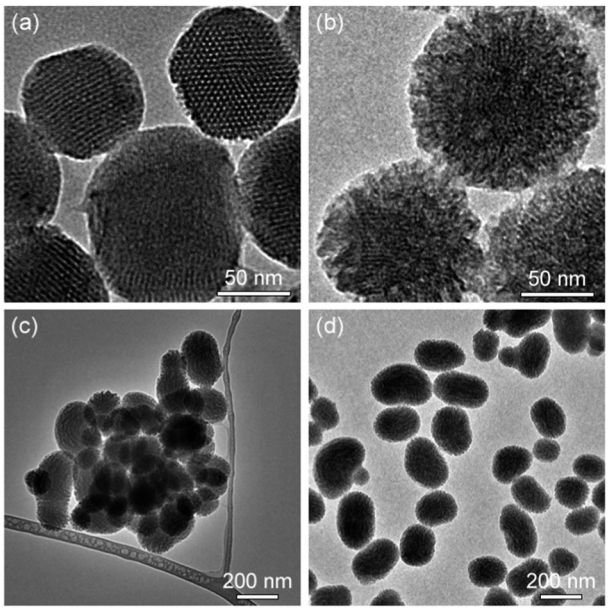

Fig. 1 TEM images of mesoporous silica nanoparticles. (a) Bare MSN, (b) and (c) O-MSN, and (d) F127-OMSN.

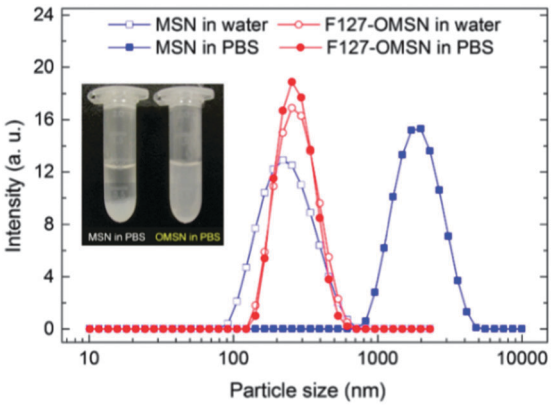

Fig. 2 Dispersibility of mesoporous silica nanoparticles in aqueous media. Size distributions of MSN and F127-OMSN in water and PBS. The inset shows the photograph of MSN (left) and F127-OMSN (right) dispersions in PBS showing the colloidal stability of PEGylated MSNs.

control experiments bare MSNs were synthesized without the addition of OTS (see ESI† for details). Fig. 1 shows TEM images of the prepared MSNs. The MCM-41 type ordered hexagonal porous structure was observed for bare MSN (Fig. 1a). Interestingly, O-MSN revealed bimodal pore structure; a randomly porous shell was observed over the MCM-41 type porous core (Fig. 1b). The shell thickness was calculated to be 12 ± 3 nm from the TEM images. Also, average sizes and size distributions of both particles were determined from TEM images and are given in Fig. S1 (ESI†). Surface area and pore volume of the particles were calculated from the adsorption–desorption data (Fig. S2, ESI†). O-MSN revealed slightly lower surface area (961.2 $m^2\ g^{-1}$) and pore volume (1.01 $cm^3\ g^{-1}$) compared to MSN (1115.7 $m^2\ g^{-1}$ and 1.25 $cm^3\ g^{-1}$). The decrease in the surface area and pore volume is the result of pore narrowing after octyl modification.[15] O-MSN formed aggregates while drying on the TEM grid, due to the hydrophobic interactions between particles (Fig. 1c). On the other hand, after coating with the pluronic polymer (F127-OMSN), particles are well dispersed on the grid (Fig. 1d) indicating the formation of the F127 coating on particles. The formation of a F127 layer on particles was further confirmed by TGA (Fig. S3, ESI†). For MSN, the weight loss at 800 °C was only 8.3% which is due to residual surfactant molecules and dehydroxylation of the silica surface.[18] For O-MSN, the weight loss reached 18.8% due to the decomposition of octyl groups. On the other hand, a large weight loss (47.1%) was observed for F127-OMSN. There are two sharp decreases in the TGA spectrum of F127-OMSN, which correspond to decomposition of F127 and octyl groups. In addition, FTIR spectra (Fig. S4, ESI†) of the particles clearly demonstrated the successful octyl modification and F127 capping (see ESI† for details) of MSNs.

Good dispersibility in biological media is vitally important for developing biocompatible and effective nanomaterials for biological applications, since aggregated particles can induce toxicity in several organs and result in poor pharmacokinetics.[19] F127-OMSN showed excellent dispersibility in both water and PBS (pH = 7.4) at a high concentration (1 mg mL^{-1}). The particle size distribution in both media was almost identical and the average particle size was around 280 nm (Fig. 2). The good aqueous dispersibility of F127-OMSN in highly salted media is attained by non-ionic and hydrophilic PEG blocks. On the other hand, MSN was fairly dispersible in water at 1 mg mL^{-1}, with slightly broader size distribution than F127-OMSN and the average particle size of around 235 nm (Fig. 2). However, MSN easily aggregated and precipitated in highly salted PBS media in a couple of minutes at the same concentration (Fig. 2 inset). Therefore, a more dilute solution (0.1 mg mL^{-1}) was used to retard the particle precipitation and particle size distribution of MSN in PBS was determined. Even at this low concentration MSN formed large aggregates and exhibited a broad particle size distribution with a large average particle size of ~2 μm (Fig. 2). To test the stability of the F127 coating, we precipitated the particles, removed the supernatant and redispersed them in PBS; this cycle was repeated ten times. The average particle size almost remained intact after the washing cycles (Fig. S5, ESI†). The good stability of the F127 layer is due to the strong hydrophobic interaction between octyl groups of O-MSN and the hydrophobic PPO block of the F127, which is stronger than either hydrogen bonding or electrostatic interactions in highly salted solutions.[10]

In order to evaluate the *in vitro* cytocompatibility of the particles 3-(4,5-dimethylthiazol-2-yl)-2,5-diphenyl-tetrazolium bromide (MTT) cytotoxicity assay was used between particle concentrations of 0.1 and 1 mg mL^{-1}. Fig. 3a indicates that both MSN and F127-OMSN are highly compatible with MCF-7 (human breast cancer cell line) cells after incubation times of 24 or 48 h.

Blood compatibility of nanomaterials is a crucial issue when they are applied by intravenous injection, a commonly applied route for drug delivery.[7,20] It is well known that interaction of MSNs with blood constituents may cause serious toxicity such as hemolysis of red blood cells (RBCs) and blood clot formation (thrombogenicity).[6,21] Therefore, we investigated the hemolytic activity and thrombogenicity of MSNs and F127-OMSN using a hemolysis assay[6] and measuring their activated partial thromboplastin time (aPTT) and prothrombin time (PT).[21] Hemolytic activity of the particles was monitored by measuring light absorption

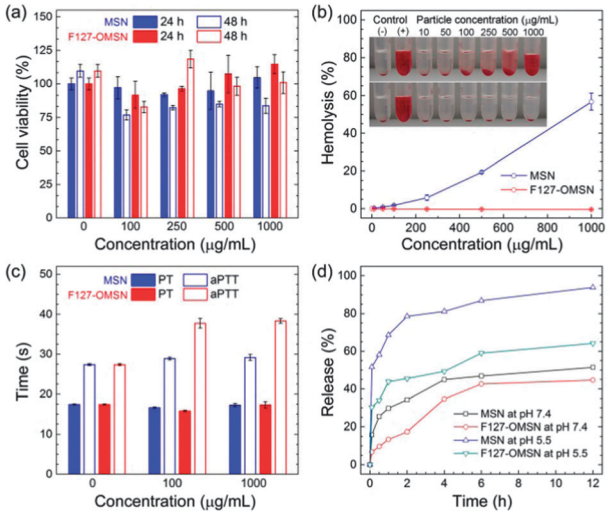

Fig. 3 (a) Cell viability results of MSN and F127-OMSN after 24 and 48 h. (b) Hemolysis results of MSN and F127-OMSN. The inset shows photographs of RBCs treated with MSN (up) and F127-OMSN (down) at different concentrations. (c) PT and aPTT values of particles. (d) DOX release profiles MSN and F127-OMSN at different pH values.

(at 570 nm) of released hemoglobin from the lysed RBCs. MSN revealed significant hemolytic activities of 5.8% at 0.25 mg mL^{-1} and 56.8% at 1 mg mL^{-1} (Fig. 3b). Strong electrostatic interaction between negatively charged silanol groups and positively charged trimethyl-ammonium head groups of the membrane lipids can cause membranolysis of RBCs.[20] Capping the MSNs with uncharged F127 molecules completely prevented the hemolytic activity even at high particle concentration (1 mg mL^{-1}) by blocking the electrostatic interaction of silanol groups with the RBC membrane (Fig. 3b). Also, the photograph of the MSN treated RBCs shows the hemoglobin (red colour) released to the supernatant, whereas no red colour was observed for F127-OMSN treated cells (Fig. 3b, inset). PT and aPTT tests are applied to investigate extrinsic and intrinsic blood coagulation pathways, respectively. The PT and aPTT results of the particles at low (0.1 mg mL^{-1}) and high (1 mg mL^{-1}) concentrations revealed that all the values are in their normal range (Fig. 3c).[21] It is well known that some dry and porous silica materials can activate the coagulation cascade due to their high absorption capacities.[21] On the other hand, the pores of the MSN and F127-OMSN are already filled with PBS, which significantly decreases the absorption capacity of particles and results in the observed anticoagulant behaviour of the particles.[20,21]

Cargo loading and release studies were performed using a cancer drug, doxorubicin (DOX). We calculated a DOX loading capacity of 15.3 μg mg^{-1} for MSN. For O-MSN, we observed a slightly lower loading efficiency (11.5 μg mg^{-1}) under the same conditions which is most likely due to the lower surface area and pore volume of octyl modified particles. The powder of DOX loaded O-MSNs was directly capped with F127 in PBS (pH 7.4) and used in drug release studies. We observed slower release profiles for F127-OMSN under both acidic (pH 5.5) and neutral (pH 7.4) conditions compared to MSN (Fig. 3d). For instance, at pH 5.5 MSN released 93.9% of its load in 12 hours, on the other hand, 64.2% DOX release was observed for F127-OMSN under the same conditions. The F127 polymer layer around the particles slows down the DOX release rate by acting as a diffusion barrier against cargo release from the pores. Also, at pH 5.5 faster DOX release was observed for both particles compared to that at pH 7.4, which is in good accordance with the previous reports.[22] The slow rate of DOX release from F127-OMSN can provide more effective therapy by preserving desired drug concentration in the body for longer times.

In conclusion, we have developed a facile method to prepare cargo loaded and PEGylated MSNs using a pluronic F127 block copolymer and hydrophobic MSNs. F127 molecules self-assembled onto the surface of hydrophobic MSNs. The resulting structures revealed good dispersibility and stability in highly salted media, in which uncoated MSNs were easily aggregated and precipitated. F127 capped MSNs demonstrated good cytocompatibility with MCF-7 cells and RBCs. Also, we did not observe any abnormality in aPTT and PT values of F127-OMSN treated blood samples. Furthermore, we demonstrated the preparation of cargo loaded and PEGylated MSNs using the pluronic capping approach. We believe that the simple PEGylation method demonstrated in this study is an excellent candidate for developing biocompatible silica based nanocarriers and theranostic agents.

This work was supported by the TUBITAK Grant No. 111T696. M.B. acknowledges partial support from the Turkish Academy of Sciences (TUBA).

Notes and references

1 S. H. Wu, Y. Hung and C. Y. Mou, *Chem. Commun.*, 2011, **47**, 9972–9985.
2 J. E. Lee, N. Lee, T. Kim, J. Kim and T. Hyeon, *Acc. Chem. Res.*, 2011, **44**, 893–902.
3 K. Yamashita, Y. Yoshioka, K. Higashisaka, K. Mimura, Y. Morishita, M. Nozaki, T. Yoshida, T. Ogura, H. Nabeshi and K. Nagano, *et al.*, *Nat. Nanotechnol.*, 2011, **6**, 321–328.
4 S. Sharifi, S. Behzadi, S. Laurent, M. L. Forrest, P. Stroeve and M. Mahmoudi, *Chem. Soc. Rev.*, 2012, **41**, 2323–2343.
5 Q. He, Z. Zhang, Y. Gao, J. Shi and Y. Li, *Small*, 2009, **5**, 2722–2729.
6 Y. S. Lin and C. L. Haynes, *J. Am. Chem. Soc.*, 2010, **132**, 4834–4842.
7 T. Yu, K. Greish, L. D. McGill, A. Ray and H. Ghandehari, *ACS Nano*, 2012, **6**, 2289–2301.
8 D. Tarn, C. E. Ashley, M. Xue, E. C. Carnes, J. I. Zink and C. J. Brinker, *Acc. Chem. Res.*, 2013, **46**, 792–801.
9 Z. Tao, M. P. Morrow, T. Asefa, K. K. Sharma, C. Duncan, A. Anan, H. S. Penefsky, J. Goodisman and A.-K. Souid, *Nano Lett.*, 2008, **8**, 1517–1526.
10 S. T. Yang, Y. Liu, Y. W. Wang and A. Cao, *Small*, 2013, **9**, 1635–1653.
11 S. P. Hudson, R. F. Padera, R. Langer and D. S. Kohane, *Biomaterials*, 2008, **29**, 4045–4055.
12 Y. Teow, P. V. Asharani, M. P. Hande and S. Valiyaveettil, *Chem. Commun.*, 2011, **47**, 7025–7038.
13 Q. He, J. Zhang, J. Shi, Z. Zhu, L. Zhang, W. Bu, L. Guo and Y. Chen, *Biomaterials*, 2010, **31**, 1085–1092.
14 Z. N. Wu, C. R. Guo, S. Liang, H. Zhang, L. P. Wang, H. C. Sun and B. Yang, *J. Mater. Chem.*, 2012, **22**, 18596–18602.
15 V. Cauda, A. Schlossbauer, J. Kecht, A. Zurner and T. Bein, *J. Am. Chem. Soc.*, 2009, **131**, 11361–11370.
16 A. Yildirim, H. Budunoglu, B. Daglar, H. Deniz and M. Bayindir, *ACS Appl. Mater. Interfaces*, 2011, **3**, 1804–1808.
17 S. Febvay, D. M. Marini, A. M. Belcher and D. E. Clapham, *Nano Lett.*, 2010, **10**, 2211–2219.
18 L. T. Zhuravlev, *Langmuir*, 1987, **3**, 316–318.
19 L. S. Wang, L. C. Wu, S. Y. Lu, L. L. Chang, I. T. Teng, C. M. Yang and J. A. Ho, *ACS Nano*, 2010, **4**, 4371–4379.
20 A. Yildirim, E. Ozgur and M. Bayindir, *J. Mater. Chem. B*, 2013, **1**, 1909–1920.
21 Q. He, J. Zhang, F. Chen, L. Guo, Z. Zhu and J. Shi, *Biomaterials*, 2010, **31**, 7785–7796.
22 Y. Gao, Y. Chen, X. Ji, X. He, Q. Yin, Z. Zhang, J. Shi and Y. Li, *ACS Nano*, 2011, **5**, 9788–9798.

Supplementary Information

Pluronic polymer capped biocompatible mesoporous silica nanocarriers

Adem Yildirim,*[ab] Gokcen Birlik Demirel,[bc] Rengin Erdem, [ab] Berna Senturk, [ab] Turgay Tekinay,[ab] and Mehmet Bayindir*[abd]

[a]*Institute of Materials Science and Nanotechnology,* [b]*UNAM-National Nanotechnology Research Center, Bilkent University 06800 Ankara, Turkey. E-mail: ademy@bilkent.edu.tr*
[c]*Department of Chemistry, Gazi University, 06500 Ankara, Turkey.*
[d]*Department of Physics, Bilkent University, 06800 Ankara, Turkey;*
E-mail: bayindir@nano.org.tr

We have provided experimental details and general procedures, particle size distributions, surface area and pore volume analysis, TGA and FTIR results, and effect of washing on average particle size.

S1. Experimental Section

Materials

Tetraetyl orthosilicate (TEOS), octyltriethoxysilane (OTS), sodium hydroxide, ammonium nitrate, and hydrofluoric acid (HF) were purchased from Merck (Germany), cetyltriammoniumbromide (CTAB), pluronic polymer (F127), ethanol, hydrochloric acid (37%) (HCl), and doxorubicin hydrochloride (DOX) were purchased from Sigma-Aldrich (U.S.A.), dimethyl sulphoxide (DMSO), methanol, and isopropanol (IPA) were purchased from Carlo-Erba (Italy), and tetrahydrofuran (THF) was purchased from Labkim (Turkey). All chemicals were used as purchased.

Synthesis of MSNs

To synthesize OMSN, first 200 mg CTAB and 5 mg F127 were dissolved in 96 mL of deionized water and 0.7 mL of 2 M NaOH was added. Then the reaction mixture was heated to 80 °C while stirring vigorously (600 rpm) and 1 mL of TEOS was rapidly added under vigorous stirring (600 rpm). After 90 min, to prepare the octyl containing shell, 0.25 mL of OTS was dissolved in 10 mL THF and slowly added to the reaction mixture. The mixture was further stirred for 3 h. Finally, reaction mixture was cooled down to the room temperature, particles were collected by centrifugation at 9000 rpm for 20 min and washed with ethanol twice. Surfactant molecules were extracted by stirring the particles in 50 mL of 20 g L^{-1} ethanolic ammonium nitrate at 60 °C for 30 min. This treatment repeated twice to ensure complete surfactant removal. Particles were washed with methanol twice afterwards and dried at 50 °C overnight. MSN was synthesized without the addition of OTS; other parameters were same with the O-MSN synthesis.

F127 capping of O-MSN

25 mg of O-MSN was dispersed in 50 mL of F127 solution in water (5 mg/mL) by sonication and stirring. The dispersion sonicated for 15 min and afterwards stirred vigorously for 1 h. F127 capped particles were precipitated at 9000 rpm for 20 min and redispersed in 50 mL of F127 solution in water (5 mg/mL). Aforementioned sonication and stirring steps were repeated. Finally, particles were precipitated and washed with water or phosphate-buffered saline (PBS) twice to remove the excess F127 molecules.

Cell Culture

Human breast adenocarcinoma cells (MCF-7) were grown to confluence at 37 °C under 5 % CO_2 in Dulbecco's Modified Eagle Serum (DMEM) containing 1% penicillin/streptomycin, 10 % fetal bovine serum (FBS) and 2 mM L-glutamine.

Cytotoxicity assay in vitro

Cells in the logarithmic growth phase were washed once with PBS, trypsinized and resuspended in fresh medium. The cells were seeded in 96-well plates at 5 x 10^3 cells/well. After 24 h of culture, the medium was removed by aspiration and replaced with 100 µL of fresh medium containing MSN or F127-OMSN at concentrations of 100, 250, 500 or 1000 µg/mL and incubated for 24 or 48 h. The cytotoxicity of particles was determined by the 3-(4,5-dimethyl-2-thiazolyl)-2,5-diphenyltetrazolium bromide (MTT) reduction assay (Sigma, Aldrich). At least two well columns containing cells without the particles were used as a negative control. MTT reagent (5 mg mL^{-1}) containing medium was added to each well, and the plates were incubated in the dark for 4 h at 37°C. After incubation, medium was removed and the resulting purple formazan crystals were dissolved by adding medium. Then the optical density was measured at 570 and 680 nm by using a microplate reader (SpectraMax, M5). The optical density of wells containing untreated cells was considered as 100 %. All the experiments were performed in triplicate.

Hemolysis assay

EDTA stabilized human blood samples were collected from volunteers at Bilkent University Health Center (Ankara, Turkey). Fresh blood samples (3 mL) were centrifuged at 1600 rpm for 5 min and RBCs were obtained after removing the blood plasma. Precipitated RBC pellet was washed five times with 6 mL of PBS and RBCs were dispersed in 25 mL of PBS. 0.2 mL of RBCs were placed in plastic vials and 0.8 mL of MSN or F127-OMSN solutions in PBS at different concentrations were added. Also, positive and negative control samples were prepared by adding 0.8 mL of water and PBS, respectively. The samples were incubated at room temperature for 2 h. Samples were slightly shaken once for every 30 min to resuspend the RBCs and MSNs. After incubation, RBC were precipitated at 1600 rpm and 200 µL of supernatants was transferred to a 96-well plate to measure the absorbance of released hemoglobin, from damaged RBCs, with a microplate reader at 570 nm. Absorbance at 655

nm was recorded as reference. Hemolysis percentages of the RBCs were calculated using the following formula;

% Hemolysis = (abs of sample-abs of negative control) / (abs of positive control-abs of negative control)

Percent hemolysis values were calculated from three separate experiments.

Blood clotting assay

For PT and aPTT measurements, human blood samples were collected to citrate stabilized vials from volunteers. Plasma samples were freshly prepared from the blood samples and immediately used in the experiments. 50 µL of MSN or F127-OMSN solutions in PBS were added to the 450 µL of plasma samples, and incubated for 5 min at 37 °C. Final particle concentrations in the resulting solutions were 0.1 and 1 mg/mL. After incubation, particles were removed by centrifugation and 50 µL portions of supernatants were used to measure PT and aPTT values using a semi-automatic blood coagulation analyzer (Tokra Medikal, Ankara, Turkey). Also, control measurements were performed using 50 µL PBS. All PT and aPTT values were calculated from three separate measurements.

DOX loading and release experiments

In order to load DOX into the pores of MSN or O-MSN, 10 mg of particles were dispersed in 1 mL of DOX solution (7.5 mg mL^{-1}) in ethanol and shook at 300 rpm for 24 h. Then the particles were collected by centrifugation. DOX loaded MSNs were washed with water twice to remove the non-adsorbed DOX molecules. For O-MSN before precipitation 5 mg of F127 added into the solution. DOX loaded OMSN were transferred into the water as described above to produce DOX loaded F127-OMSN. The amounts of adsorbed DOX were determined by monitoring the fluorescence of DOX at 590 nm (excitation wavelength is 488 nm) after etching the silica in 1.2 % HF solution for overnight.

DOX release profiles of MSN and F127-OMSN was determined by dispersing 5 mg of particles in 8 mL of PBS at pH 7.4 or pH 5.5 and each solution were separated to 10 eppendorf tubes. The tubes were shaken at 37 °C for 12 h and at different time intervals one tube removed and centrifuged. The volumes of supernatants were completed to 20 mL and fluorescence peak of DOX at 590 nm was monitored using a fluorescence spectrophotometer

in order to determine the released DOX amount.

Characterization

Transmission electron microscopy (TEM) images were taken using a Tecnai G2 F30 (FEI) microscope. Average particle sizes of MSNs were measured with Zetasizer Nanoseries (Malvern Instruments). Surface area and pore volume of the particles were determined using iQ-C (Quantachrome). Before measurements, all samples were degassed at 150 ºC for 24 h. Thermal gravimetric analyses (TGA) were performed with Q500, (TA Instruments). Fourier transform infrared (FTIR) spectra of particles were recorded by using a Fourier transform infrared spectrometer (FTIR, Vertex 70, Bruker). Optical absorption measurements in cytotoxicity and hemolysis assays were carried out using a Microplate reader (Spectramax M5, Molecular Devices). Fluorescence of DOX was measured using a Fluorescence Spectrophotometer (Eclipse, Varian).

S2. Particle size distributions

Average particle sizes of MSN and O-MSN was calculated to be 107 ± 27 nm and 149 ± 39 nm, respectively.

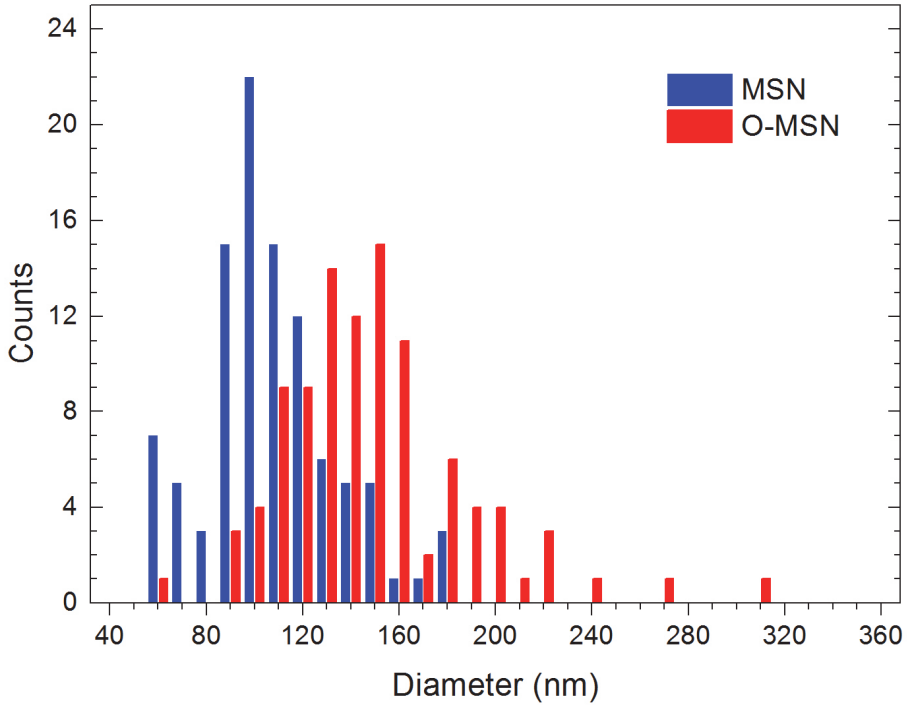

Fig. S1 Particle size distributions of MSN and O-MSN which were calculated according to the TEM images. Octyl modification significantly increased particle size indicating octyl containing shell formation.

S3. Nitrogen adsorption and desorption curves

Surface area and pore volume of the particles were calculated from nitrogen adsorption/desorption curves using Brunauer-Emmett-Teller (BET) theory and Density Functional Theory (DFT), respectively.

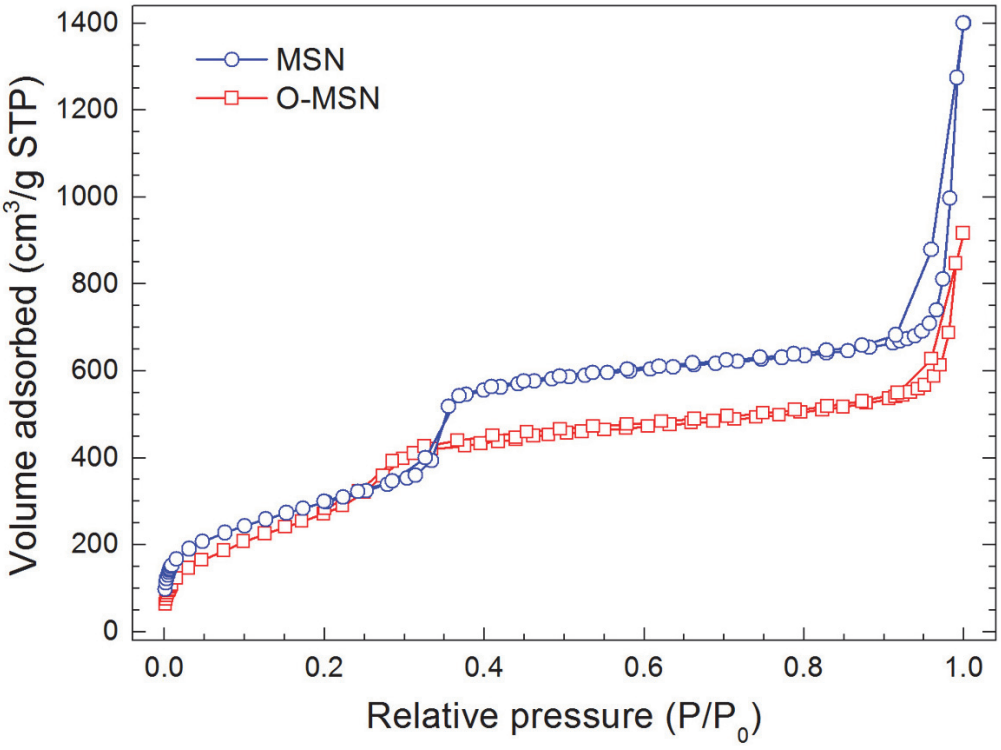

Fig. S2 Nitrogen adsorption and desorption curves of MSN and O-MSN. Octyl addition slightly reduced the surface area and pore volume of the particles.

S4. TGA Analysis

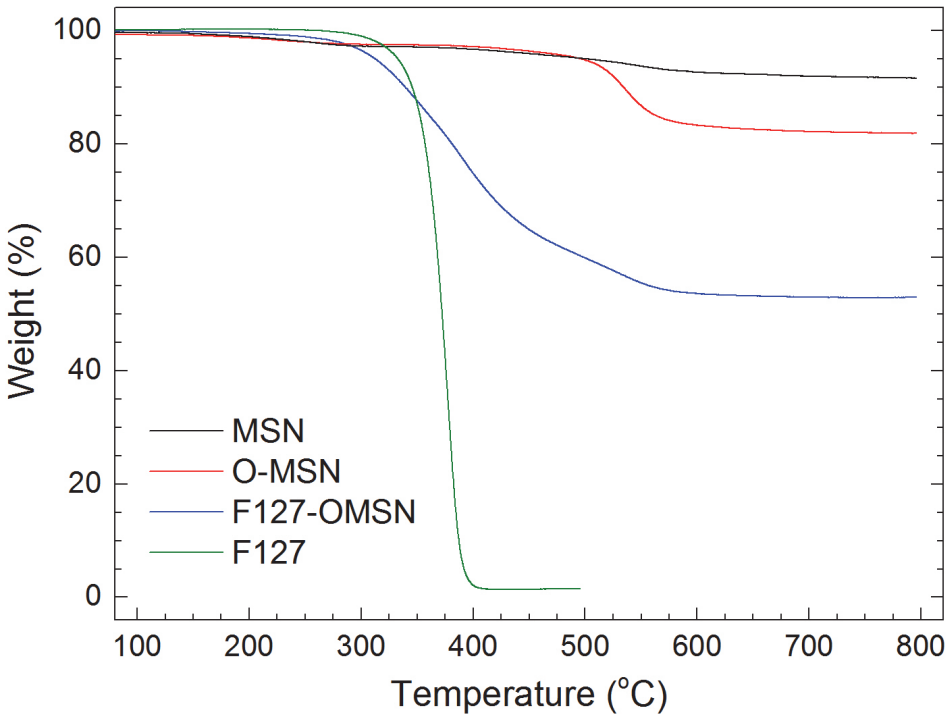

Fig. S3 TGA spectra of MSN, O-MSN, F127-OMSN and F127 polymer. After octyl addition and F127 capping weight loss of the particles gradually increased proving the formation of octyl and F127 layer around MSNs.

S5. FTIR Analysis

Several infrared absorption bands of F127 polymer is clearly observable in the FTIR spectrum of F127-OMSN; CH_2 stretch (2880 cm^{-1}), CH_2 scissor (1464 cm^{-1}), CH_2 wag (2880 cm^{-1}), CH_2 twist (1234 cm^{-1}), proving the capping of OMSN with the F127 polymer (Fig. S4).[1,2] The broad absorption band around 2900 cm^{-1} in the FTIR spectrum of OMSN indicating the presence of octyl groups. Also, some weak CH_2 absorption bands were observed in the bare MSN spectrum, which is due to the presence of residual surfactants; CTAB and F127.

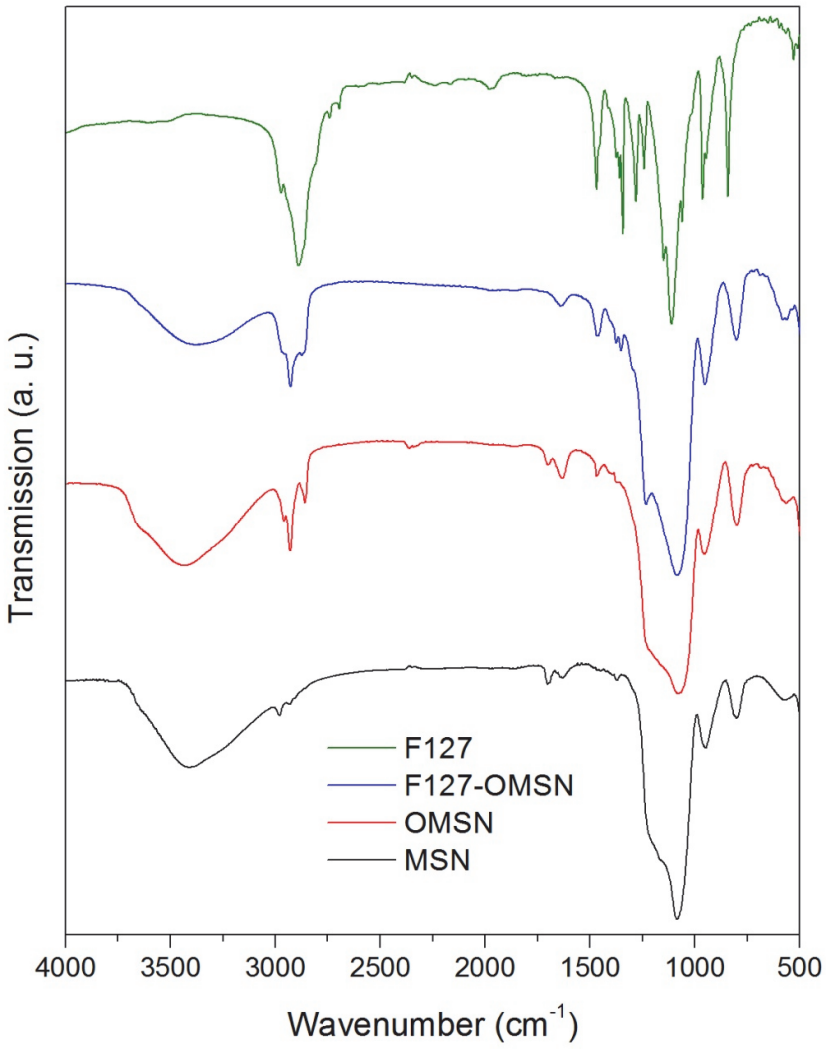

Fig. S4 FTIR spectra of MSN, O-MSN, F127-OMSN and F127 polymer showing successful octyl modification and F127 capping of particles.

S6. Stability of F127 coating

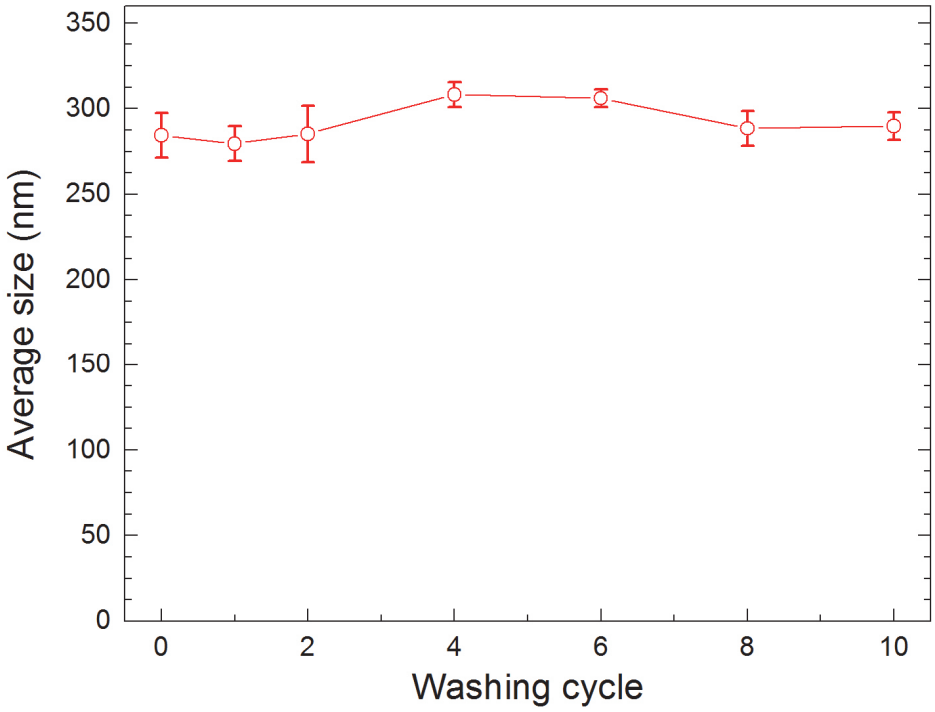

Fig. S5 The average zeta size of F127-OMSN in PBS after several washing cycles. Even after 10 washing cycles average particle size remained almost intact indicating the good stability of self-assembled pluronic layer.

References

(1) C. Guo, H. Liu, J. Wang and J. Chen, *J. Colloid Interface Sci.*, 1999, **209**, 368-373.

(2) Y. L. Su, J. Wang, and H. Z. Liu, *Langmuir*, 2002, **18**, 5370-5374.